Recent Results from the Daya Bay Reactor Neutrino Experiment

Yiming Zhang[a]
(on behalf of the Daya Bay collaboration)
Department of Engineering Physics, Tsinghua University, Beijing, China

The Daya Bay reactor neutrino experiment has presented several new results about neutrino and reactor physics with the full detector configuration after more data collection and better reassessment of systematics. I would introduce the latest progress made by the experiment in this talk, including the neutrino oscillation analysis both using neutron capture on gadolinium (nGd) and using neutron capture on hydrogen (nH), their combination, a search for a light sterile neutrino and a measurement of the reactor antineutrino flux and spectrum. The newest nGd analysis gave $\sin^2 2\theta_{13} = 0.084 \pm 0.005$ and $|\Delta m^2_{ee}| = (2.42 \pm 0.11) \times 10^{-3} eV^2$, while the newest nH analysis gave $\sin^2 2\theta_{13} = 0.071 \pm 0.010$.

1 Introduction

Neutrino flavor oscillations are caused by the misalignment between neutrino flavor and mass eigenstates. The transformation between the three favour eigenstates $(\nu_e, \nu_\mu, \nu_\tau)$ and mass eigenstates (ν_1, ν_2, ν_3) is done by the Pontecorvo-Maki-Nakagawa-Sakata (PMNS) 3×3 unitary matrix. It is parameterised by three mixing angles $\theta_{12}, \theta_{23}, \theta_{13}$ and one CP-violation phase δ_{CP}.

The Daya Bay experiment was designed to measure the value of θ_{13} observing disappearance of reactor anti-neutrinos due to flavour oscillations. The survival probability is:

$$P(\bar{\nu_e} \to \bar{\nu_e}) = 1 - \sin^2 2\theta_{13} \sin^2(\frac{\Delta m^2_{ee} L}{4E}) - \cos^4 \theta_{13} \sin^2 2\theta_{12} \sin^2(\frac{\Delta m^2_{21} L}{4E}) \quad (1)$$

where E is anti-neutrino energy, L is the propagation distance, $\Delta m^2_{12} = m^2_2 - m^2_1$ is the difference of squared masses and the definition and derivation of Δm^2_{ee} can be found here[1].

In 2012, the Daya Bay collaboration has published the first non-zero results with a significance of 5.2 standard deviations [2]. After the experimental confirmation of a non-zero θ_{13}, measurements of the Dirac phase, δ_{CP} , which is related to CP violation of leptonic sector, and the sign of Δm^2_{32}, are the next major goals in neutrino oscillation physics. To reach the next milestone, the precision of θ_{13} is important and need to be improved.

2 Daya Bay Experiment

The Daya Bay reactor neutrino experiment is located next to six commercial nuclear reactors, each of which has a nominal thermal power of 2.9 GW. The experiment consists of two near halls and one far hall. The power-weighted baselines to the six power reactors are about 500 m and 1.7 km for the near and far halls, respectively. Each near hall has two antineutrino detectors (ADs) and the far hall has four ADs. Details of the detector design could be found here[3,4]. The

[a] ym-zhang12@mails.tsinghua.edu.cn

reactor electron antineutrinos were detected by the inverse beta decay (IBD) interactions, where the neutron in the final state can be either captured on gadolinium (nGd) or on hydrogen (nH). The neutrino fluxes and energy spectra measured with the far site ADs were compared with the measurements at the near sites and/or reactor predictions. Deficits and distortions were observed.

Two sets of data of the Daya Bay experiments have been taken. The first set of data is 217 days taken from Dec. 2011 to Jul. 2012 with only six ADs installed and the second set of data is 404 days taken from Oct. 2012 to Dec. 2013 with all eight ADs installed and running. The operation history of the Daya Bay experiment, number of IBD events accumulated in the near and far detectors and the measured value of $\sin^2 2\theta_{13}$ as a function of time is shown in Figure 1. The experiment will continue operation until 2017, by the end of which more than 4 million IBD events will be recorded.

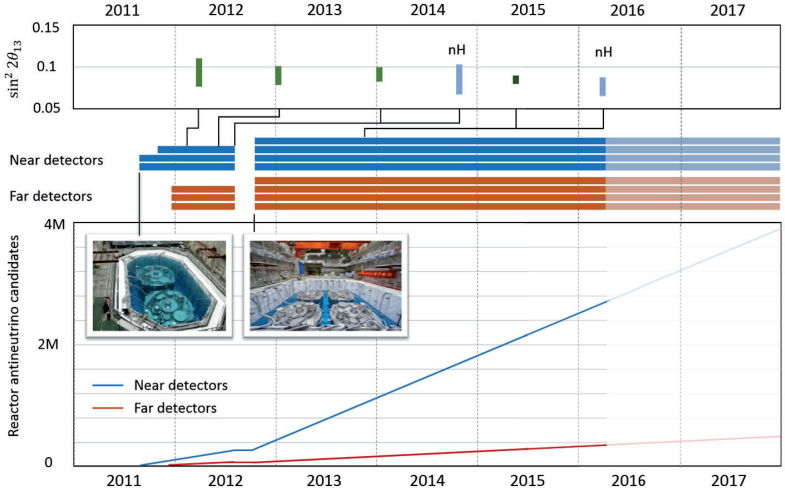

Figure 1 – Operation history of the Daya Bay Experiment and the measured values of $\sin^2 2\theta_{13}$.

2.1 Antineutrino Detector Design

Each of the eight functionally identical antineutrino detectors consists of three zones separated by acrylic vessels. The inner zone is the antineutrino target containing 20 tons of Gadolinium-loaded liquid scintillator (GdLS). The middle zone is the gamma catcher containing 22 tons of liquid scintillator (LS). The outer zone, filled with 36 tons of mineral oil (MO), shields background radiations. There are 192 8" PMTs mounted on eight ladders in each AD. To improve the light collection, there are two reflectors on the top and bottom of the outer acrylic vessel. On the top of each AD there are three automatic calibration units (ACUs), each containing three sources, LED,^{68}Ge and $^{241}Am-^{13}C+^{60}Co$. Calibrations are performed once a week.

2.2 Muon Veto System

The muon veto system consists of a water pool instrumented with PMTs as the Cerenkov detectors and 4 layers of RPC tracking detectors. The former is composed of the inner water shield (IWS) and outer water shield (OWS), to detect cosmic ray muons and to shield neutrons and gammas from rock. All the ADs are put inside the water pools fore each hall. The latter covers

the water pool to provide further muon tracking information. The water Cerenkov detector efficiency is greater than 99.7% for long track muon.

2.3 Detector Response

Many calibration sources (ACU sources, ^{137}Cs, ^{54}Mn, ^{40}K, Am-Be and Pu-C neutron sources) and environmental natural sources (^{40}K, ^{208}Tl and neutron capture on H, C and Fe) were used to measure the energy resolution and study the non-linearity of detector response. The energy resolution is $7.5/\sqrt{E_{vis}/MeV}$. The non-linearity of detector response, caused by the liquid scintillator (including quenching effect and Cerenkov yield) and the readout electronics characteristics, has a minimal impact on the oscillation angle measurement, but is more relevant for the measurement of the reactor antineutrino mass difference and the absolute reactor flux. The energy response model is obtained semi-empirically and is compared with various gamma sources and ^{12}B beta-decay spectrum (nominal response). A cross check is done with fit to ^{208}Th, ^{212}Bi, ^{214}Bi beta-decay spectrum and also the Michel electron. The energy non-linearity uncertainty could be within 1% for the energy above 2 MeV, as shown in Figure 2.

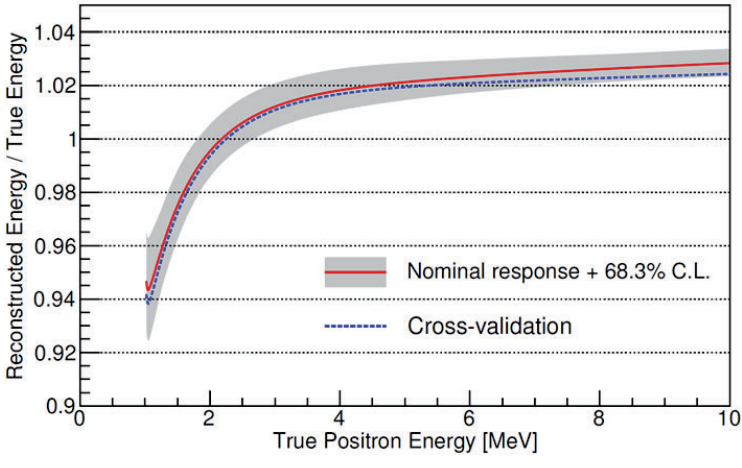

Figure 2 – Energy non-linearity nominal response and validation

3 Anti-neutrino detection and backgrounds

Anti-neutrinos are detected via inverse beta decay (IBD) $\bar{\nu_e} + p \rightarrow e^+ + n$. Positron energy losses and the energy from its annihilation form the so-called "prompt" signal. It takes some time for the neutron to thermalise. It is eventually captured either on gadolinium with a lifetime of $30\mu s$ releasing about 8 MeV γ-cascade or on hydrogen with a lifetime of $200\mu s$ releasing single 2.2 MeV γ. The neutron capture constitutes the so-called "delayed" signal which is used in coincidence with the prompt signal to select IBD candidates.

The IBD selection procedure begins by removing unphysical events caused by flashing PMTs. For the IBD sample selected based on neutrons captured on gadolinium, a coincidence within 1-200 μs of two events with energies 0.7-12 MeV and 6-12 MeV is required. Different categories of muon veto are applied. In order to remove any possible ambiguities in the pair selection procedure we require no other events within and around the coincidence window.

For the IBD sample selected based on neutrons captured on hydrogen, the coincidence window is 400 μs and the energies cuts are 1.5-12 MeV and 3σ region around the fitted nH

peak. The distance between the prompt and delayed signals is required to be within 500 mm, to improve the signal/background ratio.

The most important background is accidental background which are from single events and 'accidentally' pass the IBD event selection. The second effective backgrounds are from cosmic ray muons. Muon-induced products, such as fast neutron and $^9Li/^8He$, can mimic IBD as a correlated pair. For the fast neutron case, neutron scattering followed by neutron capture could mimic the IBD event. For the $^9Li/^8He$ background, the prompt signals are from the beta-decay and the delayed signals are from neutron capture. The calibration source, AmC, in ACU is another background source.

4 Recent results

4.1 Three-Flavor Neutrino Oscillation Analysis Using nGd

With 217 days of 6-AD and 404 days of 8-AD data, the best oscillation analysis result is shown in Figure 3. By analyzing the relative antineutrino fluxes and energy spectra between the near and far detectors, it was got that $\sin^2 2\theta_{13} = 0.084 \pm 0.005$ and $|\Delta m^2_{ee}| = (2.42 \pm 0.11) \times 10^{-3} eV^2$ in the three-neutrino framework.

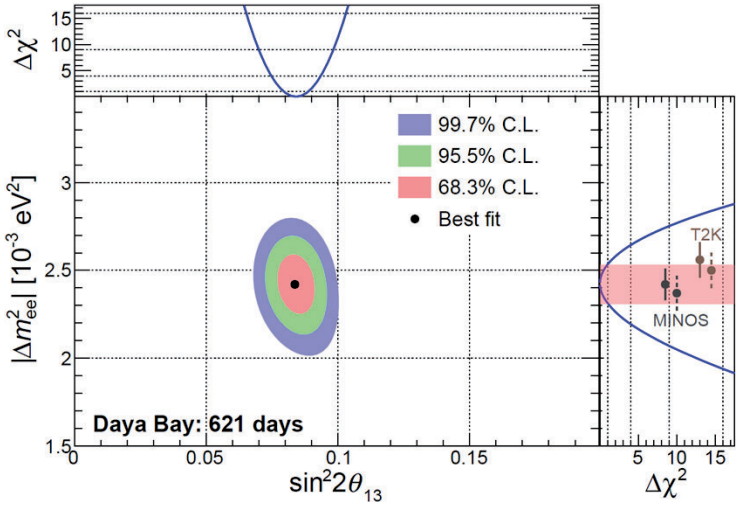

Figure 3 – Regions in the $|\Delta m^2_{ee}| - \sin^2 2\theta_{13}$ plane allowed at the 68.3%, 95.5% and 99.7% confidence levels by the near-far comparison of $\bar{\nu}_e$ rate and energy spectra. The best estimates were $\sin^2 2\theta_{13} = 0.084 \pm 0.005$ and $|\Delta m^2_{ee}| = (2.42 \pm 0.11) \times 10^{-3} eV^2$ (black point). The adjoining panels show the dependence of $\Delta\chi^2$ on $\sin^2 2\theta_{13}$ (top) and $|\Delta m^2_{ee}|$ (right). The $|\Delta m^2_{ee}|$ allowed region (shaded band, 68.3% C.L.) was consistent with measurements of $|\Delta m^2_{ee}|$ using muon disappearance by the MINOS[5] and T2K[6] experiments, converted to $|\Delta m^2_{ee}|$ assuming the normal (solid) and inverted (dashed) mass hierarchy.

The electron antineutrino survival probability as a function of the ratio of the effective propagation distance L_{eff} over the average antineutrino energy $\langle E_\nu \rangle$ is shown in Figure 4 . More details about this result can be found in [1].

4.2 Independent θ_{13} Measurement using nH

The detection of inverse beta decays can also be tagged by neutron capture on hydrogen. The antineutrino events for hydrogen capture are quite distinct from those for gadolinium capture with largely different systematic uncertainties, allowing a determination independent of the nGd

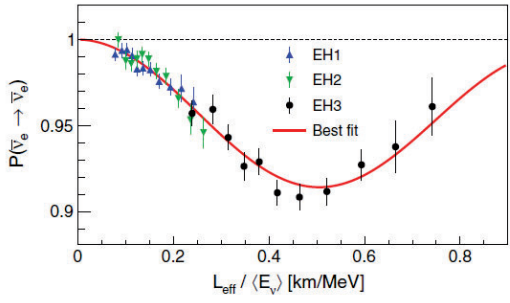

Figure 4 – Electron antineutrino survival probability versus effective propagation distance L_{eff} divided by the average antineutrino energy $\langle E_\nu \rangle$.

result and an improvement on the precision of θ_{13} measurement. Using the same 621 days data sample as the most recent nGd oscillation analysis[1], the latest independent θ_{13} measurement using nH sample was published[7] just after the 51st Rencontres de Moriond EW 2016. This nH analysis is based on the rate information. The best-fit value for both the normal and inverted neutrino-mass hierarchies is $\sin^2 2\theta_{13} = 0.071 \pm 0.010$, with a χ^2 per degree of freedom of 6.3/6.

For a combination of the most recent nGd-IBD result of $\sin^2 2\theta_{13} = 0.084 \pm 0.005$ and the nH-IBD result, both the analytical calculation and simultaneous fit resulted in $\sin^2 2\theta_{13} = 0.082 \pm 0.004$, which is an 8% improvement in precision. Figure 5 shows the ratio of the measured rate to the predicted rate assuming no oscillation, for each detector.

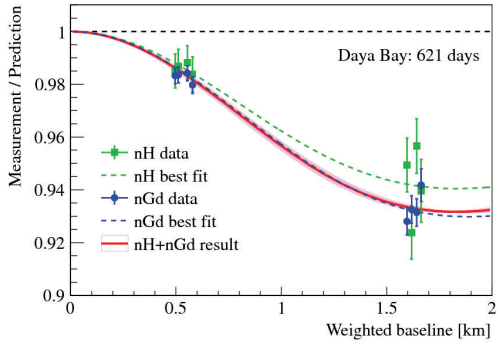

Figure 5 – Ratio of measured to predicted IBD rate in each detector assuming no oscillation *vs.* flux-weighted baseline. Each detector is represented with a green square (blue circle) for the nH (nGd) analysis. Error bars include statistical, detector-related, and background uncertainties. The dashed green (blue) curve represents the neutrino oscillation probability using the nH (nGd) result for $\sin^2 2\theta_{13}$ and the global fit value of Δm^2_{32} (the nGd result for Δm^2_{ee}). The solid red curve represents the oscillation probability using the nH-nGd combined result and Δm^2_{32}, and the magenta error band is the uncertainty of Δm^2_{32}. The baselines of EH1-AD2 and EH2-AD2 are shifted by +20 m, and those of EH3-AD1, 2, 3, and 4 are shifted by -30, -10, +10, and +30 m, respectively, for visual clarity.

4.3 Search for a Light Sterile Neutrino

With the first 217 days of data a search for light sterile neutrino mixing was performed [8]. The experiment has multiple baselines from the six antineutrino detectors to the six nuclear reactors, and this unique feature makes it possible to test for oscillations to a fourth (sterile) neutrino. The study showed that the relative spectral distortion observed was consistent with that of the three-flavor oscillation model and the most stringent limit was set at $10^{-3}eV^2 < |\Delta m^2_{41}| < 0.1eV^2$. The excluded region for $\sin^2 2\theta_{14}$ and $|\Delta m^2_{41}|$ can be seen in Figure 6, where the most of it had not been explored before.

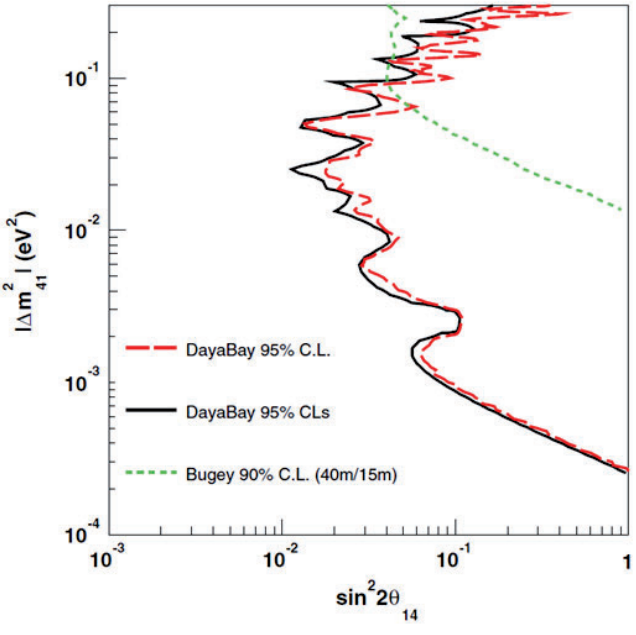

Figure 6 – Exclusion contours for the neutrino oscillation parameters $\sin^2 2\theta_{14}$ and $|\Delta m^2_{41}|$. Normal mass hierarchy is assumed for both Δm^2_{31} and Δm^2_{41}. The red long-dashed curve represents the 95% C.L. exclusion contour with Feldman-Cousins method. The black solid curve represents the 95% CLs exclusion contour. The parameter space to the right side of the contours is excluded. For comparison, Bugeys[9] 90% C.L. limits is also shown as the green dashed curve. The figure is from [8].

4.4 Measurement of the Reactor Antineutrino Flux and Spectrum

A new measurement of the neutrino flux and energy spectrum of electron antineutrinos from the six 2.9 GW_{th} nuclear reactors was reported [10]. With the 217 days of data, the IBD yield was measured to be $(1.55\pm0.04)\times10^{18}cm^2/GW/day$ or $(5.92\pm0.14)\times10^{43}cm^2/fission$. The ratio of the flux to the prediction made with the Huber+Mueller (ILL+Vogel) fissile antineutrino model is $0.946 \pm 0.022(0.991 \pm 0.023)$ and it agrees with results reported by previous short-baseline reactor antineutrino experiments, as seen in Figure 7. At the energy region of 4-6 MeV, a bump was observed with a local significance of around 4σ.

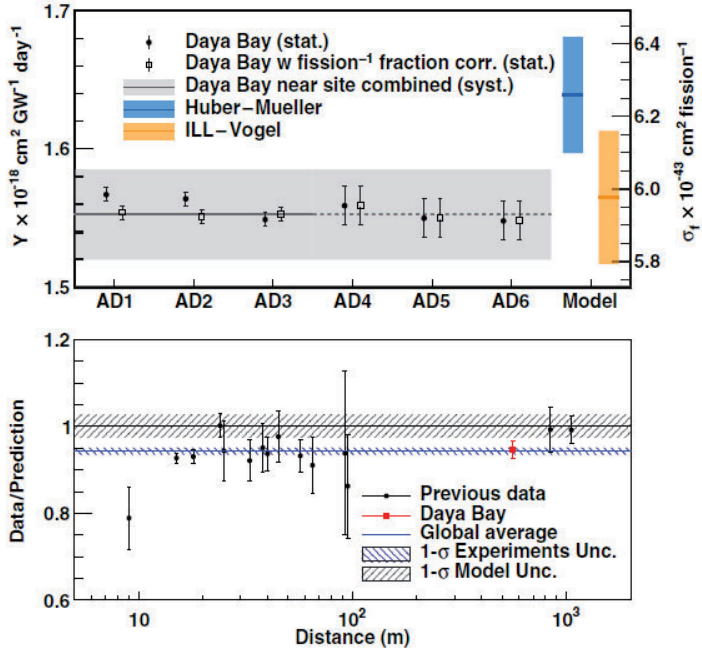

Figure 7 – The measured reactor $\bar{\nu}_e$ rate as a function of the distance from the reactor, normalized to the theoretical prediction with the Huber+Mueller model. The rate is corrected for 3-flavor neutrino oscillations at each baseline. The blue shaded region represents the global average and its 1σ uncertainty. The 2.7% model uncertainty is shown as a band around unity. Measurements at the same baseline are combined for clarity. The Daya Bay measurement is shown at the flux-weighted baseline (573 m) of the two near halls. The figure is from [10].

5 Summary

The Daya Bay Neutrino Experiment provides the most precise measurement of $\sin^2 2\theta_{13}$ to date and measures the oscillation frequency Δm^2_{ee} with a precision comparable to that of accelerator experiments. The experiment investigated possible existence of light sterile neutrinos, and set limits in the $10^{-3}eV^2 < |\Delta m^2_{41}| < 0.1eV^2$ region, which was previously unexplored. The experiment reproduced the previously observed disagreement with predictions in the measurement of the total flux and spectrum shape of the reactor $\bar{\nu}_e$s. At the energy region of 4-6 MeV, a bump was observed with a local significance of around 4σ.

Acknowledgments

Daya Bay is supported in part by the Ministry of Science and Technology of China, the U.S. Department of Energy, the Chinese Academy of Sciences, the National Natural Science Foundation of China, the Guangdong provincial government, the Shenzhen municipal government, the China General Nuclear Power Group, Key Laboratory of Particle Physics and Radiation Imaging (Tsinghua University), the Ministry of Education, Key Laboratory of Particle Physics and Particle Irradiation(Shandong University), the Ministry of Education, Shanghai Laboratory of Particle Physics and Cosmology, the Research Grants Council of the Hong Kong Special Administrative Region of China, the University Development Fund of The University of Hong

Kong, the MOE program for Research of Excellence at National Taiwan University, National Chiao-Tung University, and NSC fund support from Taiwan, the U.S. National Science Foundation, the Alfred P. Sloan Foundation, the Ministry of Education, Youth, and Sports of the Czech Republic, the Joint Institute of Nuclear Research in Dubna, Russia, the CNFC-RFBR joint research program, the National Commission of Scientific and Technological Research of Chile, and the Tsinghua University Initiative Scientific Research Program. We acknowledge Yellow River Engineering Consulting Co., Ltd., and China Railway 15th Bureau Group Co., Ltd., for building the underground laboratory. We are grateful for the ongoing cooperation from the China General Nuclear Power Group and China Light and Power Company.

References

1. F. P. An et al. [Daya Bay Collaboration], Phys. Rev. Lett. 115, 111802 (2015).
2. F. P. An et al. [Daya Bay Collaboration], Phys. Rev. Lett. 108, 171803 (2012).
3. F. P. An et al. [Daya Bay Collaboration], Nucl. Instrum. Methods A 685, 78-97 (2012).
4. F. P. An et al. [Daya Bay Collaboration], Nucl. Instrum. Methods A 811, 133-161 (2016).
5. P. Adamson et al. [MINOS Collaboration], Phys. Rev. Lett. 112, 191801 (2014).
6. K. Abe et al. [T2K Collaboration], Phys. Rev. Lett. 112, 181801 (2014).
7. F. P. An et al. [Daya Bay Collaboration], Phys. Rev. D 93, 0720 (2016).
8. F. P. An et al. [Daya Bay Collaboration], Phys. Rev. Lett. 113, 141802 (2014).
9. Y. Declais et al. Nucl. Phys. B 434, 503 (1995).
10. F. P. An et al. [Daya Bay Collaboration], Phys. Rev. Lett. 116, 061801 (2016).